

Flow noise from spoilers in ducts

Cheuk Ming Mak^{a)} and Jia Wu

Department of Building Services Engineering, The Hong Kong Polytechnic University, Hung Hom, Kowloon, Hong Kong, China

Chao Ye

Department of Building Services Engineering, The Hong Kong Polytechnic University, Hung Hom, Kowloon, Hong Kong, China and State Key Laboratory of Acoustics, Institute of Acoustics, Chinese Academy of Sciences, Beijing 100080, China

Jun Yang

State Key Laboratory of Acoustics, Institute of Acoustics, Chinese Academy of Sciences, Beijing 100080, China

(Received 17 April 2008; revised 28 March 2009; accepted 10 April 2009)

Measurements of flow noise produced by strip spoilers in the air duct of a ventilation system and radiated from an open exhaust termination unit into a reverberation chamber have been made. The results agree with the previous work of Nelson and Morfey [J. Sound Vib. **79**, 263–289 (1981)]. Prediction of flow noise produced by multiple spoilers requires the values of the ratio of the mean drag forces that act on the spoilers, the phase relationship between the fluctuating drag forces that act on the spoilers, and the coherence function of the noise sources. The latter is empirically derived from the measured results, where the predicted results agree well with the experimental results within 3 dB at most frequencies except for very high frequencies.

© 2009 Acoustical Society of America. [DOI: 10.1121/1.3127129]

PACS number(s): 43.50.Nm, 43.50.Ed, 43.50.Cb, 43.28.Ra [JWP]

Pages: 3756–3765

I. INTRODUCTION

Flow noise is produced by in-duct elements such as dampers, sensors, bends, transition pieces, duct corners, branch points, or even splitter attenuators. At long distances from the fans in an air duct, flow noise produced by in-duct elements can be very serious. Our objective is to enable the prediction of the level and spectral content of the flow noise that is produced by the multiple elements in the air duct of a ventilation system.

The current design guides that are usually adopted, such as the ASHRAE handbook¹ and the CIBSE guide,² provide design methods for the prediction of flow noise only from a single, isolated in-duct element in an air ductwork system. Wilson and Iqbal³ observed that these methods seriously underestimate the levels of flow noise in practical systems.

Measured data that have been reported in previous studies^{4–9} can only be used with confidence on systems that incorporate the same configurations and carry the same airflows. Attempts^{10–12} based on simplified theories that have been made using the limited data and equations are not applicable to systems with very different configurations.

Gordon^{13,14} conducted a series of experiments and produced a free-field scaling law radiation model relating the sound power radiated from an element to the geometrical and flow parameters involved to collapse his measured sound power data into a “generalized spectrum.” However, the experimental results he obtained were at low Strouhal numbers

and high Mach numbers that are different from the air duct flow in a ventilation system (at high Strouhal numbers and low Mach numbers). Heller and Widnall¹⁵ clarified the acoustical significance of the duct that encloses the noise source.

A method for predicting flow noise was produced and verified experimentally (at high Strouhal numbers and low Mach numbers) by Nelson and Morfey.¹⁶ Oldham and Ukpoho¹⁷ then rewrote the Nelson–Morfey equations. They determined the appropriate values of the open area ratio and of the characteristic dimension to be applied to a flow spoiler in a circular or a square duct. They focused on the sound field that is due to a single duct element such as a strip spoiler. Flow noise can be produced by the interaction of a moving fluid with a single duct element or a combination of duct elements. Ukpoho and Oldham¹⁸ experimented with two sound sources (in-duct spoilers) to find that the flow noise increases when two duct elements are considered and that this increase is frequency-dependent. The latter conclusion shows that it is intuitively the same as the two sources in the active control of the sound in an air duct. Owing to the flow interaction between the duct elements,¹⁹ the random (partially coherent) field case is likely to be the general case in ventilation systems. Mak and Yang^{20,21} applied a model of partially coherent sources to formulate the sound power level due to duct spoilers. This model considers the acoustic interaction of two in-duct spoilers based on the earlier work of Nelson and Morfey.¹⁶ Mak²² later modified the Mak–Yang equations to determine the sound power radiated by the interaction of more complicated spoilers in circular ducts. He assumed a coherence function and compared the measured

^{a)}Author to whom correspondence should be addressed. Electronic mail: becmmak@polyu.edu.hk

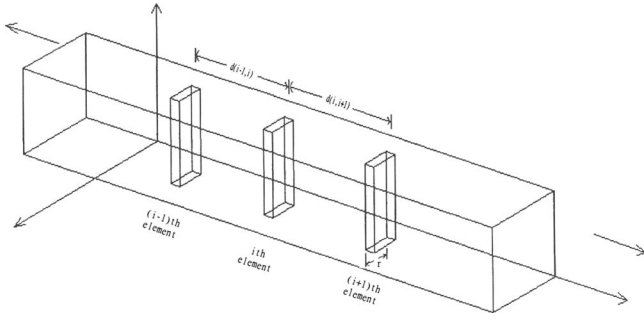


FIG. 1. Three in-duct elements in an infinite air duct.

values of Ukpo and Oldham¹⁸ with the predicted values of the modified Mak–Yang equations and found that these predicted values agreed well with the general trend of the measured values. Mak and Oldham’s^{23,24} approach was later used to modify the Mak–Yang equations to produce a turbulence-based prediction technique for flow noise.²⁵ Recent work by Mak and Au²⁶ has confirmed the usefulness of the approach. Mak²⁷ then extended Mak and Yang’s prediction method to the prediction of multiple flow noise sources.

Airflow, acoustic, and force measurement data are collapsed into normalized spectra with the aid of these derived predictive equations. This is a prediction technique for the flow-generated noise produced by multiple spoilers in the air duct of a ventilation system.

II. THEORY AND PREDICTIVE EQUATIONS OF NOISE PRODUCED BY IN-DUCT FLOW SPOILER(S)

Mak adopted the concept of partially coherent sound fields to formulate the sound powers that are produced by the interaction of multiple spoilers at frequencies below and above the cut-on frequency of the lowest transverse duct mode. An example of three flow spoilers in an infinite air duct is shown in Fig. 1.

Two equations were obtained to determine the sound power that is generated by the interaction of multiple spoilers, one of which corresponds to frequencies, f_c , below the cut-on frequency, f_0 , and one of which corresponds to frequencies above it. For N ($N > 2$) elements, the following are derived. For $f_c < f_0$,

$$\Pi_N = K^2(S) \times \Gamma_1 \times I_1. \quad (1)$$

For $f_c > f_0$,

$$\Pi_N = K^2(S) \times \Gamma_2 \times I_2. \quad (2)$$

The power term Γ_1 from the first spoiler below the cut-on frequency is

$$\Gamma_1 = \{\rho_0 A [\sigma^2 (1 - \sigma)]^2 C_D^2 U_c^4 / 16 c_0\}.$$

The power term Γ_2 from the first spoiler above the cut-one frequency is

$$\Gamma_2 = \{\rho_0 \pi A^2 (S)^2 [\sigma^2 (1 - \sigma)]^2 \times [C_D^2 U_c^6 / 24 c_0^3 r^2] \times [1 + (3\pi c_0 / 4\omega_c)(a + b)/A]\}.$$

The interaction term I_1 below the cut-on frequency is

$$I_1 = \left\{ \sum_{i=1}^N \xi_i^2 + 2 \sum_{i=1}^{N-1} \sum_{j=1}^{N-2} \left[\sqrt{\gamma_{i(i+1)}^2} \times \cos(\omega_c d_{i(i+1)} / c_0) \cos[\phi_{i(i+1)}(\omega_c)] \xi_i \xi_{i+1} + \sqrt{\gamma_{(i-1)(i+j)}^2} \times \cos(\omega_c d_{(i-1)(i+j)} / c_0) \times \cos[\phi_{(i-1)(i+j)}(\omega_c)] \xi_{i-1} \xi_{i+j} \right] \right\}.$$

The interaction term I_2 above the cut-on frequency is

$$I_2 = \left\{ \sum_{i=1}^N \xi_i^2 + 2 \sum_{i=1}^{N-1} \sum_{j=1}^{N-2} \left[\sqrt{\gamma_{i(i+1)}^2} Q_{i(i+1)} \times \cos[\phi_{i(i+1)}(\omega_c)] \xi_i \xi_{i+1} + \sqrt{\gamma_{(i-1)(i+j)}^2} Q_{(i-1)(i+j)} \cos[\phi_{(i-1)(i+j)}(\omega_c)] \xi_{i-1} \xi_{i+j} \right] \right\},$$

where $N > 2$, N , i , and j are integers and $j = 1, 2, \dots, (N-2)$.

In the above equation, a value is ignored if any one of its subscripts is zero or greater than N . $Q_{i(i+1)}$ is given by $Q_{i(i+1)} = \Omega_{i(i+1)} / \Psi_{i(i+1)}$, where

$$\Omega_{i(i+1)} = \frac{k^2 ab}{6\pi} 3 \left[\frac{\sin e}{e} + \frac{2 \cos e}{e^2} - \frac{2 \sin e}{e^3} \right] + \frac{k(a+b)}{8} 2 \left[J_0(e) - \frac{J_1(e)}{e} \right],$$

$$\Psi_{i(i+1)} = \left[\frac{k^2 ab}{6\pi} + \frac{k(a+b)}{8} \right],$$

and $e = kd_{i(i+1)}$.

$Q_{(i-1)(i+j)}$ is given by $Q_{(i-1)(i+j)} = \Omega_{(i-1)(i+j)} / \Psi_{(i-1)(i+j)}$, where

$$\Omega_{(i-1)(i+j)} = \frac{k^2 ab}{6\pi} 3 \left[\frac{\sin e}{e} + \frac{2 \cos e}{e^2} - \frac{2 \sin e}{e^3} \right] + \frac{k(a+b)}{8} 2 \left[J_0(e) - \frac{J_1(e)}{e} \right],$$

$$\Psi_{(i-1)(i+j)} = \left[\frac{k^2 ab}{6\pi} + \frac{k(a+b)}{8} \right],$$

and $e = kd_{(i-1)(i+j)}$.

d_{ij} is the distance between the i th spoiler and the j th spoiler; k is the wave number; J_0 and J_1 are the zero- and first-order Bessel’s functions, respectively; a and b are the duct cross-section dimensions; r is a characteristic dimension of the element; A is the area of the duct cross-section by $A = (a \times b)$; A_c is the area of the duct constriction by $A_c = (a \times b - r \times b)$; U_c is the flow velocity in the constriction that is provided by the spoiler and is defined by the volume flow rate q and the area of the duct constriction A_c , such that $U_c = q / A_c = UA / A_c$; U is the mean duct flow velocity; σ is the open area ratio determined by $\sigma = A_c / A$. The Strouhal number for this duct and flow is $S = f_c r / U_c$; the factor $K(S)$ is the ratio of fluctuating to steady-state drag forces on the spoilers;

P_N is the infinite-duct values of the radiated sound power; f_0 is the cut-on frequency of the first transverse duct mode (i.e., the least non-zero value of the cut-on frequency is defined by $f_0 = (c_0/2\pi)\sqrt{(m\pi/a)^2 + (n\pi/b)^2}$, where $m, n = 0, 1, \dots$); c_0 is the ambient speed of sound; ρ_0 is the ambient air density; γ_{ij}^2 is the coherence function of the i th spoiler and the j th spoiler; ω_c is the center radiant frequency of the measurement band; $\phi_{ij}(\omega_c)$ is the phase of the cross-power spectral density of the source volume of the i th sound source and the j th sound source; ζ_i is a constant ratio of the mean drag forces acting on the i th spoiler and the first spoiler; ΔP_S is the static pressure drop across a spoiler (Pa); and C_D is the drag coefficient determined by

$$C_D = \frac{\Delta P_S}{\frac{1}{2}\rho_0 U_c^2 (1 - \sigma)}. \quad (3)$$

Comparing the above expressions with those obtained by Nelson and Morfey¹⁶ for the sound power generated by an in-duct spoiler, the interaction factor β_N can be defined as follows:

$$\beta_N = \begin{cases} I_1, & f_c < f_0, \\ I_2, & f_c > f_0. \end{cases} \quad (4)$$

Furthermore, if the sound power that is due to an in-duct spoiler is denoted as Π_S , a simple relationship between Π_N , the sound power that is due to multiple (N) spoilers and that due to a single spoiler, is then obtained as follows:

$$\Pi_N = \Pi_S \times \beta_N, \quad (5)$$

where Π_S can be obtained by using the prediction method provided by Nelson and Morfey,¹⁶ and β_N can be determined by experiments.

We define ζ_i as the constant ratio of the mean drag forces acting on the i th spoiler and the first spoiler. The first spoiler is closest to the inlet of the air flow:

$$\zeta_i = \frac{\bar{F}_{z1}}{\bar{F}_{zi}}, \quad (6)$$

where \bar{F}_{zi} is the mean drag force acting on the i th spoiler counted from the inlet of the air flow, and \bar{F}_{z1} is the mean drag force acting on the first spoiler. The mean drag force acting on the i th spoiler can be expressed as $F_{zi} = A\Delta P_S$.

Han *et al.*²⁸ and Han and Mak²⁹ suggested that the phase of the cross-power spectral density of the source volume of the i th sound source and the j th sound source, $\phi_{ij}(\omega_c)$, can be given by

$$\phi_{ij}(\omega_c) = \delta_{ij} - kM\bar{d}_{ij}, \quad (7)$$

where δ_{ij} is the difference between the phases of the total fluctuating drag forces acting on the i th spoiler and the j th spoiler: $\delta_{ij} = \theta_j(\omega) - \theta_i(\omega)$, where $\theta_i(\omega)$ and $\theta_j(\omega)$ are the phases of the fluctuating drag force acting on the i th spoiler, respectively. k is the wave number, $M = U/c_0$, and $\bar{d}_{ij} = d_{ij}/(1 - M^2)$.

The coherence functions, γ_{ij}^2 , of the noise sources are obtained as follows.

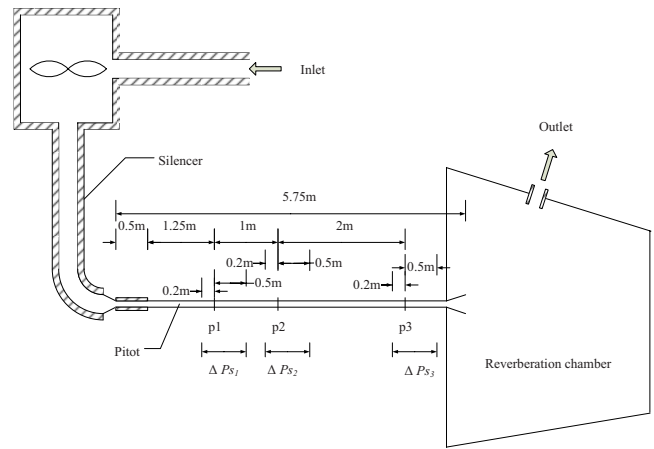


FIG. 2. (Color online) A schematic diagram of the test rig (plan view). (ΔP_{S1} , ΔP_{S2} , and ΔP_{S3} = a static pressure drop across the first spoiler, the second spoiler, and the third spoiler, respectively; p1 = position at which the first test spoiler was inserted; p2 = position at which the second test spoiler was inserted; and p3 = position at which the third test spoiler was inserted.)

III. EXPERIMENTAL PROCEDURE

A. Design of the experimental rig

The test rig used for the determination of the sound power generated by flat plate spoiler(s) and their interactions are shown in Fig. 2. Air flow was provided by a centrifugal fan driven by a variable speed motor. The fan was vibration-isolated by springs and was enclosed in a lined acoustic enclosure of $1.22 \times 1.22 \times 1.22 \text{ m}^3$. Fan noise was attenuated on both the upstream and downstream sides by silencers and acoustically lined elbows. The 0.1 m^2 test duct was made of steel and was enclosed by 25-mm-thick absorptive lining to reduce breakout noise from the duct. This arrangement yielded a quiet, fully developed air flow at the first test piece counted from the inlet of air flow, which was situated approximately 1.75 m from the duct entrance section. The total length of the duct was 5.45 m. The duct was passed into a 70 m^3 reverberation chamber with an outlet cone of $0.16 \times 0.16 \text{ m}^2$ and a length of 0.3 m for acoustic measurements. The reverberation chamber was provided with lined outlet ducts that allowed air to escape without allowing noise from outside to penetrate. The entire system was located in another 200 m^3 reverberation chamber with a closed door so that the level of sound that was measured in the system was always well above the background noise level.

B. The spoilers used in the experiment

The spoilers used in the experiment, as shown in Fig. 3, were selected to test the validity of Mak's²⁷ prediction method for multiple flow spoilers. The spoiler plates were made from 1-mm-thick steel plate. These plates were fixed by springs and force transducers between the flanges of two adjoining sections of the test duct. The gap was sealed with compressed foam rubber. The spoilers provided a rigid obstruction to the flow in the duct and were not able to vibrate significantly in the air stream. Six different spoiler geometries were tested, each with at least four duct flow velocities. Three of the spoilers were vertical strips of plate placed centrally in the air stream. Their height was that of the test duct,

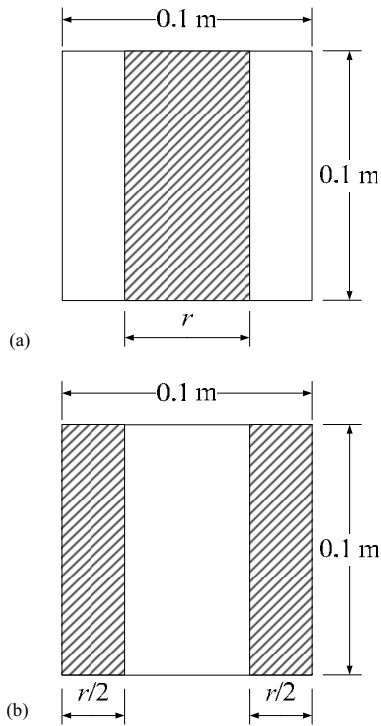


FIG. 3. Cross-section of the duct with two main types and various sizes of the flat plate strip spoilers used (shaded area). (a) Centrally placed strip spoilers; $r=0.025, 0.05, 0.075$ m. (b) The geometries consisted of trip plates protruding symmetrically from both sides of the duct, leaving a central vertical strip of the duct open; $r=0.025, 0.05, 0.075$ m.

and their widths were 0.025, 0.05, and 0.075 m, respectively. The other three geometries consisted of plates that protruded symmetrically from both sides of the duct, leaving a central vertical strip of the duct open. Again, the plates had the same height as the duct, and the widths of the two side plates were equal. The total widths in the three configurations were 0.025, 0.05, and 0.075 m, respectively. Eleven tests were conducted, as shown in Table I. In Tests 1–4, only a single spoiler was inserted into position p1. In Tests 5–9, two spoilers were inserted at two different positions p1 and p2. In Tests 10 and 11, three spoilers were inserted at three different positions p1, p2, and p3. The three spoiler positions are shown in Fig. 2.

C. Airflow measurements

The velocity profile in the empty test duct was measured.³⁰ A pitot tube was used to sample the dynamic pressure at specified points in the duct cross-section at the position shown in Fig. 4. Plots of the duct velocity profile at several test velocities at the 0.1 m side are shown in Fig. 5. The slight asymmetry of the velocity profiles that were measured is due to the non-symmetric inlet conditions and is not regarded as serious in the experiments. This procedure was used to calculate the mean duct velocity over the 5.4 m length at five duct velocities. The mean velocity calculated for each of the five velocities was found to have a linear relationship with the velocity measured at the “calibrated” position at the center of the duct (as shown in Fig. 6). Value of the mean duct velocity was determined by using this

TABLE I. Eleven spoiler configurations tested. See Fig. 2. (p1=position at which the first test spoiler was inserted, p2=position at which the second test spoiler was inserted, and p3=position at which the third test spoiler was inserted.)

LEGEND: Spoiler area, A_s
Air flow area, A_c

No.	Spoiler(s) used in the experiments	Mean flow velocities
1	$r=0.025\text{m}$ at p1	10,15,20,25,30
2	$r=0.05\text{m}$ at p1	10,14,18,22,26
3	$r=0.025\text{m}$ at p1	15,20,25,30,35
4	$r=0.05\text{m}$ at p1	10,15,20,25,30
5	$r=0.025\text{m}$ at p1 $r=0.025\text{m}$ at p2	10,15,20,25,30
6	$r=0.025\text{m}$ at p1 $r=0.05\text{m}$ at p2	10,14,18,22,26
7	$r=0.05\text{m}$ at p1 $r=0.05\text{m}$ at p2	10,13,16,19,22
8	$r=0.075\text{m}$ at p1 $r=0.075\text{m}$ at p2	10,11,12,13,14
9	$r=0.025\text{m}$ at p1 $r=0.025\text{m}$ at p2	10,14,18,22,26
10	$r=0.025\text{m}$ at p1 $r=0.025\text{m}$ at p2 $r=0.025\text{m}$ at p3	10,13,16,19,22
11	$r=0.05\text{m}$ at p1 $r=0.05\text{m}$ at p2 $r=0.05\text{m}$ at p3	10,12,14,16,18

single calibrated position of the pitot tube. The pitot tube was removed from the duct when undertaking acoustic measurements.

The static pressure drop across the various spoilers that were tested was measured using two piezometric rings located at the positions p1, p2, and p3 shown in Fig. 2. Each ring consisted of four static pressure tapings, one in each

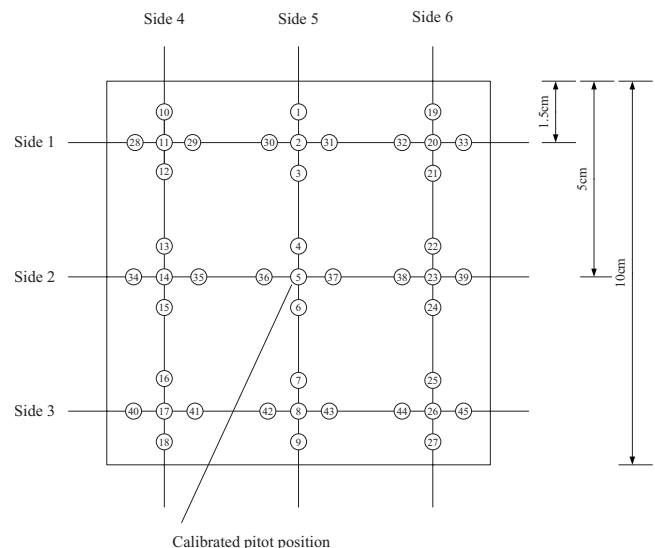


FIG. 4. Positions in the duct cross-section at which a pitot tube was used to sample the dynamic pressure.

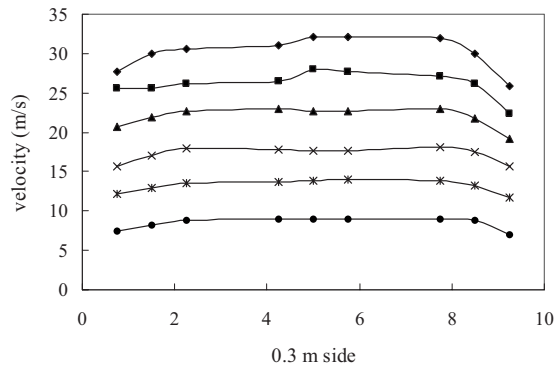


FIG. 5. (Color online) A linear relationship between the mean velocity calculated for each of the five velocities and the velocity measured at the calibrated position.

duct face. The downstream ring was far enough away (five times the duct dimensions) from the test spoiler to ensure that full static pressure recovery could take place in the wake of the flow obstructions under test.

D. Acoustic measurements

The temperature and relative air humidity in the reverberation chamber were measured with a sling psychrometer. During the measurements, the temperature ranged from 26.5 to 27.8 °C, and the relative humidity ranged from 53% to 59%. The reverberation time (RT) was measured by the impulse response method of the mean-length sequence (MLS), as shown in Fig. 7. This MLS signal was generated internally by DIRAC software installed on a notebook computer and fed to the omni-directional source B&K-type 4241, a dodecahedron loudspeaker that was placed at the corner of the chamber. A B&K-type sound level meter, which was connected to the computer through an external sound card, was located at 1.20 m above the floor at the predetermined positions. The door of the chamber was closed, and there were no personnel inside the chamber during the measurement process. Six different microphone positions were used for the frequencies between 200 and 10 kHz. All of the measured positions were located at least 1 m away from the chamber walls. The distance between the two microphones was larger than the half a wavelength of sound under consideration. The geometric mean of the measured RTs and the sound pressure

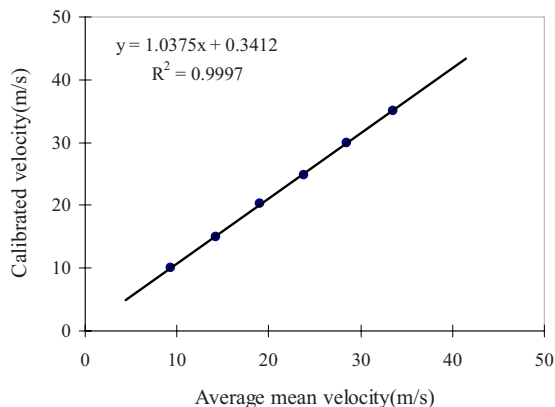


FIG. 6. Test duct velocity profile.

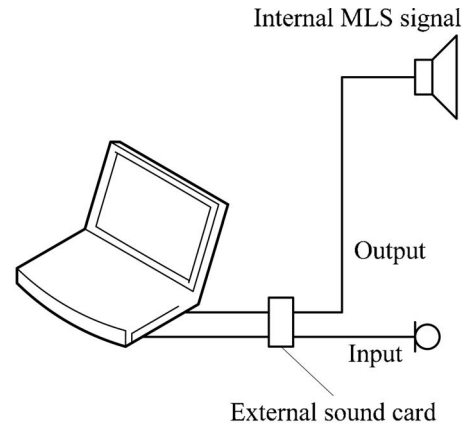


FIG. 7. A schematic diagram of the impulse response method using a MLS signal.

levels (SPLs) were based on the measured RT and the measured SPLs at the six different randomly selected positions, respectively. About 50 sampled averaged RTs and averaged SPLs were obtained so that the mean of the averaged RTs and the averaged SPLs and the standard deviation, S_D , of the variation of the averaged RTs and averaged SPLs could be calculated, respectively. Assuming that the measured value of S_D is the true standard deviation of a normal distribution of averaged RTs and averaged SPLs, it is found that the 95% confidence limits for the mean of the distribution estimated from n_s samples ($n_s=50$) are then given by $\pm 1.96S_D/\sqrt{n_s}$. The error is $\pm 1.96S_D/\sqrt{50}$, and the geometrical mean of the RTs and the SPLs should be around 1–3 s and ± 1.5 dB, respectively. The geometrical mean of the measured RT is shown in Fig. 8. The 95% confidence limits for the mean SPL are shown in Fig. 9. The results are better than those measured by Nelson and Morfey,¹⁶ as can be seen by the smaller errors at all frequencies (see Fig. 9). A sufficiently diffuse field was established in the middle of the frequency range so that more reliable results could be obtained. At high frequencies, the accuracy decreases again as the absorption in the room increases and the direct field of the duct exit encroaches on the reverberant field. The sound power level

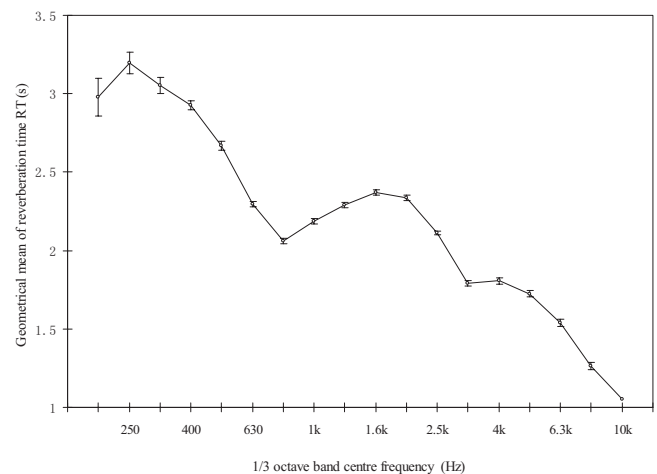


FIG. 8. Measured RTs for the test chamber and the geometrical mean of the RTs for the test chamber. Six microphone positions were used for 200 Hz–10 kHz. The error bars denote the spread of results.

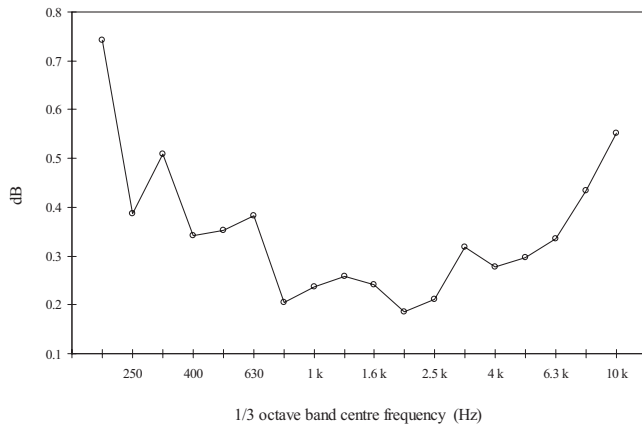


FIG. 9. The 95% confidence limits for an estimate of the mean SPL in the test chamber from the six microphone positions.

that radiated from the duct exit was then calculated from

$$SWL = SPL + 10 \log_{10} V_R - 10 \log_{10} \overline{RT} - 14,$$

where V_R is the room volume (70 m^3), \overline{RT} is the geometrical mean of the reverberation time(s), and SPL is the space-averaged sound pressure level in the chamber (dB).

The background noise due to the flow in the empty duct was monitored at five test velocities. The ambient background noise level was also measured after each test. The measured noise levels were kept at least 10 dB above the ambient level, and the background flow noise level at the given test velocity in the duct.

E. Force measurements

The arrangement of springs and force transducers is shown in Fig. 10. The plates were fixed by springs and force transducers between the flanges of the two adjoining sections of the duct, and the gap sealed with a compressed foam rubber seal. For the centrally placed strip spoiler, two transducers mounted on the duct supporting flanges were required to measure the total fluctuating drag force. For the two side strip spoilers, four transducers on the duct supporting flanges

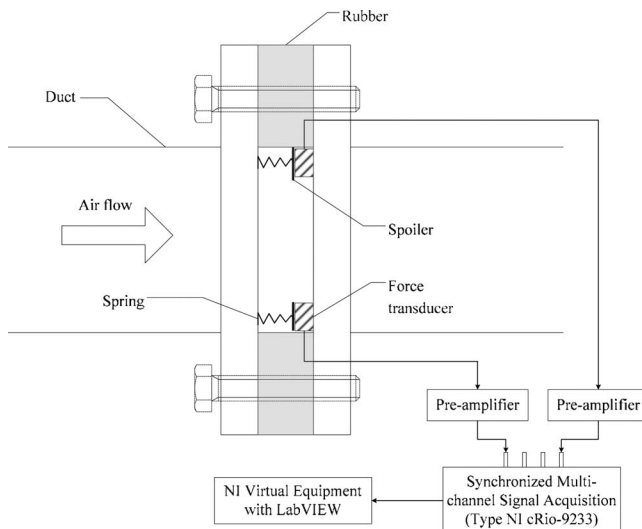


FIG. 10. A schematic diagram of the force-measuring system.

were required to measure the total fluctuating drag force. The springs used to provide support for the plates were selected to have stiffness sufficient to place the mechanical resonant frequency well below 200 Hz, the lowest 1/3 octave band measuring frequency of the reverberation chamber of 70 m^3 , and also below 50 Hz, which is the frequency of the alternating current supply in Hong Kong. The frequency response of the force transducers was flat over the measuring frequency range. Their sensitivity was 11 mV/N. The force transducers were connected to NI LABVIEW equipment via a synchronized multi-channel signal acquisition of type NI cRio-9233 through pre-amplifiers, as indicated in Fig. 10. The magnitude and phases of the total fluctuating forces acting on the spoilers at various duct flow velocities were measured in real time and converted into a frequency domain by the NI equipment.

IV. ANALYSIS AND DISCUSSION OF THE RESULTS

A. Normalization of the experimental results for a single flow spoiler

The results measured for the sound power that radiated from the end of the duct for a single spoiler can be normalized according to Nelson and Morfey.¹⁶ Their equations, and those of Mak²⁷ and Mak and Yang,^{20,21} were developed for an infinite duct. The duct used, however, was of finite length with a considerable length-absorbent lining upstream of the test duct. It has been assumed that the spoiler is transparent to the waves reflected back upstream from the duct terminations. The radiated sound power measurement has therefore been interpreted on the basis that the test duct is semi-infinite, and no compensation has been made for any subsequent re-reflection of sound arriving from the duct exit. The sound power radiated by the spoilers down one direction of the infinite duct was corrected by a power transmission loss at the duct outlet.

The drag coefficient, C_D , used in the normalization of the results for the single spoilers was evaluated from the measurements of the static pressure drop across the spoilers based on Eq. (3). The values of C_D for each spoiler were found by averaging the values calculated from the measurements of ΔP_s and U_c , at each test velocity. For most of the spoilers tested, the calculated values of C_D varied by around 0.5%–5% over the range of the test velocities used.

The result for one of the single spoilers tested, normalized¹⁶ with the measured values of C_D used and the sound power levels is shown in Fig. 11, which denotes $120 + 20 \log_{10} K(S)$ and relates to the infinite-duct values of the radiated sound power Π_N in Eqs. (1) and (2). In view of the vastly different forms of the two equations for frequencies above and below the cut-on frequency of the first transverse duct mode, the collapse of the experimental data for all of the single spoilers tested is good in view of the widely differing drag coefficients associated with the various spoilers. Nelson and Morfey¹⁶ reported that there was an error in their original normalized spectrum and that their trend lines need to be displaced vertically downwards by 6 dB. The scatter associated with the experimental points of Fig. 11 is comparable with the range of corrected trend lines in their normal-

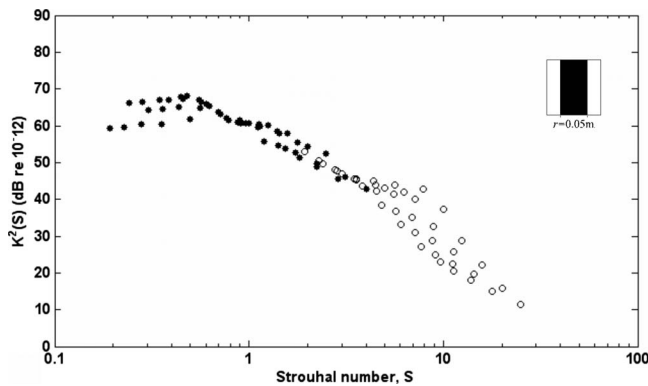


FIG. 11. Normalized 1/3 octave band results for strip spoilers in Test 2 ($r = 0.05$ m). Values of the characteristic dimension (i.e., the total strip width) r and the drag coefficient C_D , as follows. Test 2: $r = 0.05$ m, $C_D = 12.0$.

ized spectrum. This suggests that the results reported here agree well with their corrected trend lines; Fig. 12 shows a comparison of the values of the normalized results for all of the single spoilers tested and a trend line based on simple linear relationships over the range of measurements. Scattering was observed at low Strouhal numbers (or low frequencies), which was also seen in the work of Oldham and Ukpo. ¹⁷

B. Determination of the coherence function of noise sources

The assumptions used in the determination of the coherence function, γ_{ij}^2 , are as follows:

- (1) The values of the coherence function should be between 0 and 1, i.e., $0 \leq \gamma_{ij}^2 \leq 1$. If γ_{ij}^2 takes the value of 1 at certain frequencies, then this means that the i th and j th sound sources are fully coherent at those frequencies. If γ_{ij}^2 is equal to zero at certain frequencies, then this means that the i th and j th sound sources are incoherent at those frequencies.
- (2) The coherence function should be dependent on the magnitude and phases of the fluctuating drag forces acting on each spoiler at various frequencies.
- (3) The coherence function is inversely related to the distance between the i th and j th spoilers. When one flow

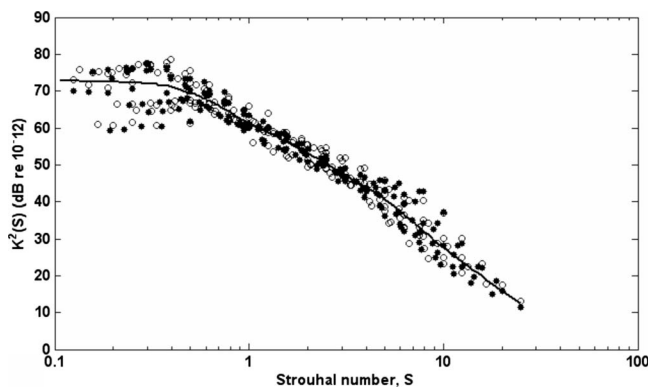


FIG. 12. The overall collapse of the normalized data for all tested single spoilers (Tests 1–4). The overall collapse of the normalized data for all single spoilers: (●) centrally placed strip spoiler; (○) plates protruding symmetrically from both sides of the duct; (—) trend line.

spoiler is far away from another, the coherence function between the flow noise sources should be small when the other parameters are fixed.

- (4) The coherence function should be dependent on the mean duct flow air velocity.

The experimental data for the two flow spoilers in Test 5 were used to obtain $\sqrt{\gamma_{ij}^2}$ in the predictive equations for multiple spoilers. The relationship between $\sqrt{\gamma_{ij}^2}$ and the other parameters, such as the phases and magnitude of the fluctuating drag forces, F , acting on the spoilers, the distance between the two noise sources, d_{ij} , and the mean flow air velocity, U , were analyzed by the Statistical Package for the Social Sciences (SPSS). The square of $\sqrt{\gamma_{ij}^2}$ will give the coherence function γ_{ij}^2 , and the value of $\sqrt{\gamma_{ij}^2}$ will therefore also be between 0 and 1.

It was found from the SPSS analysis of the data that there was an approximately linear relationship between $\sqrt{\gamma_{ij}^2}$ and $\log(|F_j(\omega)/F_i(\omega)\cos(\theta_j(\omega) - \theta_i(\omega))|)$ with a correlation coefficient of 0.84 between them. It was therefore assumed that $\sqrt{\gamma_{ij}^2}$ may be a logarithmic function that contains the factor of $|F_j(\omega)/F_i(\omega)\cos(\theta_j(\omega) - \theta_i(\omega))|$. $F_i(\omega)$ and $F_j(\omega)$ are the magnitudes of the fluctuating drag force acting on the i th and j th spoilers, respectively. To ensure that the value of the coherence function was between 0 and 1, the following preliminary formula was obtained:

$$\gamma_{ij}^2 = \log_{10}^2 \left(1 + \frac{15}{U d_{ij}} \left| \frac{F_j(\omega)}{F_i(\omega)} \right|^2 \cos^2(\theta_j(\omega) - \theta_i(\omega)) \right),$$

where $F_i(\omega)$ and $\theta_i(\omega)$ are the magnitude and phases, respectively, of the fluctuating drag force acting on the i th spoiler.

Together with the values of the other parameters, such as the phases of the cross-power spectral density of the source volumes and the ratio of the mean drag forces, the interaction factor β_N in the predictive equations can be obtained.

C. Comparison between predicted and measured results

Mak's predictive equations for multiple flow spoilers were used to predict the sound power levels produced by two or three flow spoilers in Tests 5–11. The predicted and measured results of the sound wave levels in the seven tests at a particular flow velocity are shown in Figs. 13–19. The error between the predicted and measured results was ± 0 –3 dB at most frequencies at a particular mean flow velocity. The deviation between the predicted and measured results at certain frequencies at or above 4 kHz at a particular flow may have been due to high frequency vibration modes of the flow spoiler or the duct system.

These predictive equations developed are useful for predicting the level and spectral contents of the flow-generated noise from multiple in-duct flow spoilers at the design stage. This prediction provides a normalized spectrum, using a table of parameters derived from experimental model measurements.

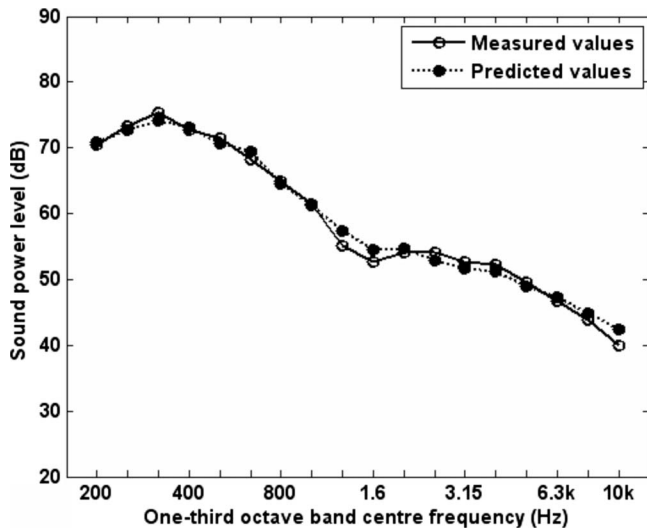


FIG. 13. Comparison of the measured values and predicted values of the SPL in Test 5 at $U=20$ m/s.

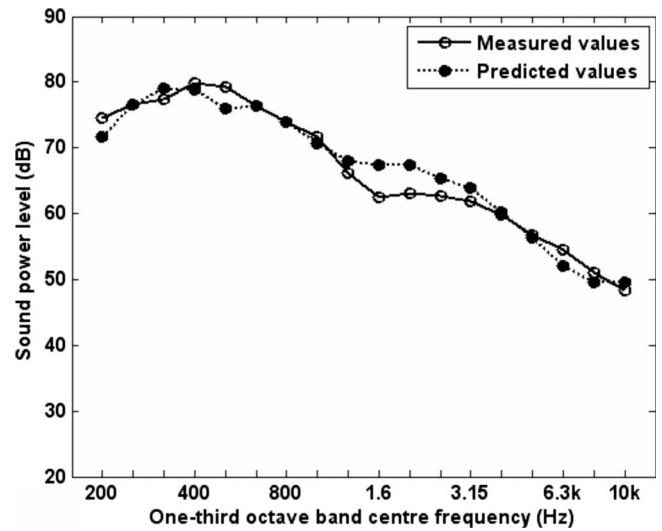


FIG. 16. Comparison of the measured values and predicted values of the SPL in Test 8 at $U=11$ m/s.

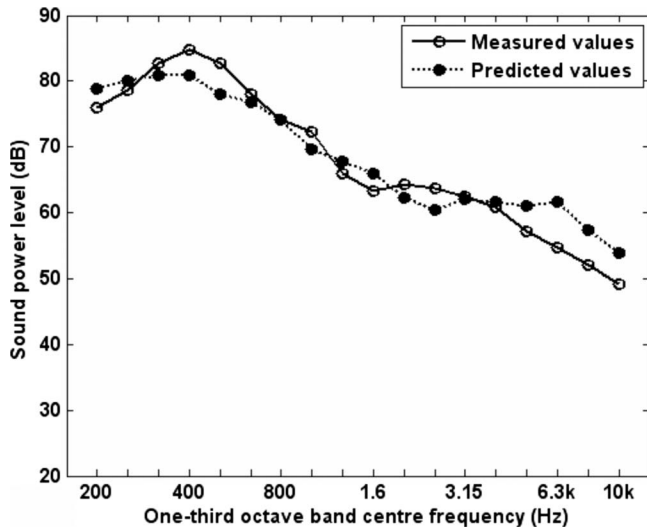


FIG. 14. Comparison of the measured values and predicted values of the SPL in Test 6 at $U=22$ m/s.

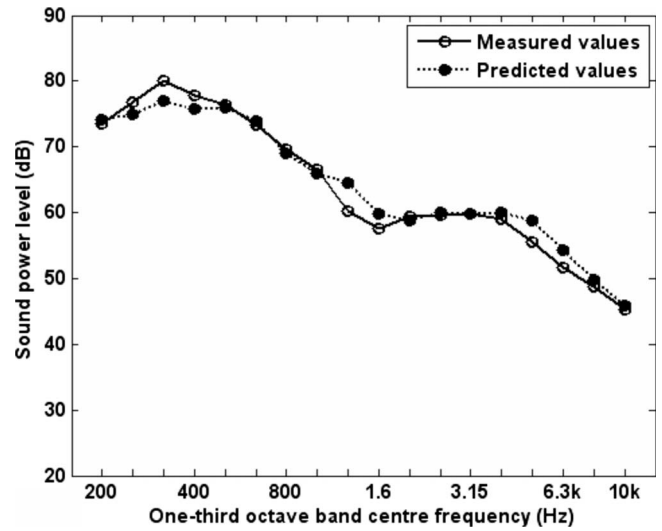


FIG. 17. Comparison of the measured values and predicted values of the SPL in Test 9 at $U=18$ m/s.

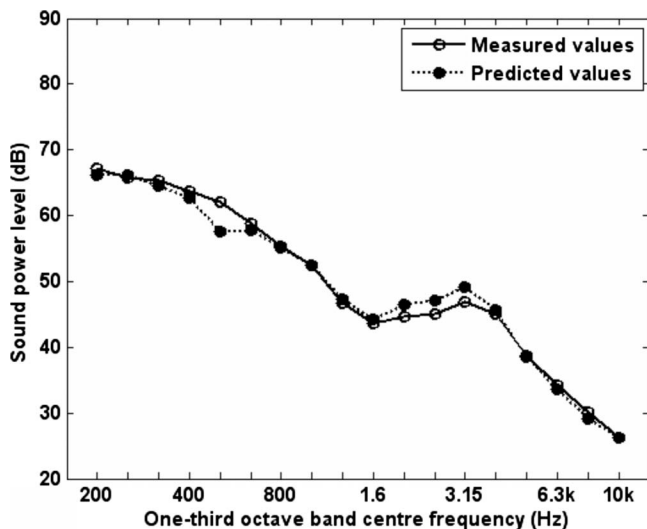


FIG. 15. Comparison of the measured values and predicted values of the SPL in Test 7 at $U=10$ m/s.

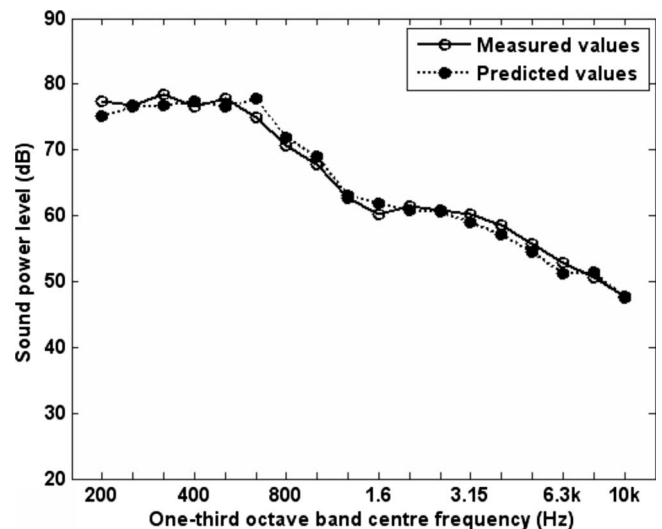


FIG. 18. Comparison of the measured values and predicted values of the SPL in Test 10 at $U=19$ m/s.

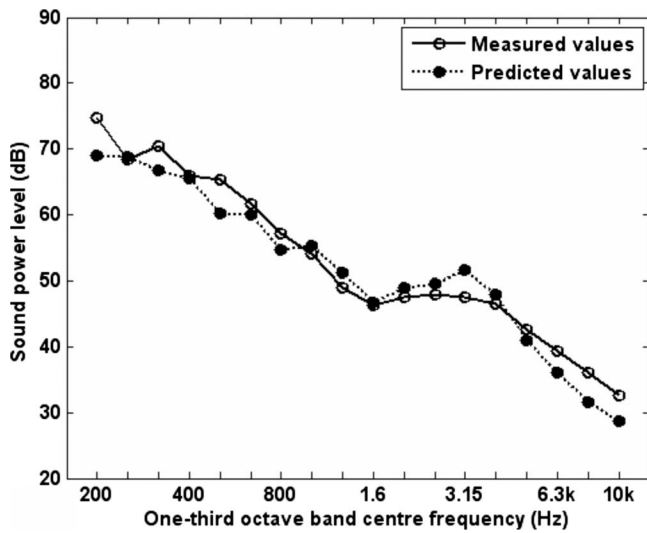


FIG. 19. Comparison of the measured values and predicted values of the SPL in Test 11 at $U=10$ m/s.

V. CONCLUSION

The collapse of the data found with single flow spoilers is similar to that observed by Nelson and Morfey¹⁶ and Oldham and Ukpho.¹⁷ Together with the normalized spectrum and the coherence function, Mak's predictive equations²⁷ for multiple flow spoilers, one can now predict the sound power levels produced by two or three flow spoilers at most frequencies at various mean duct flow velocities.

It is suggested that the line trends reported in this study, together with the coherence function of the noise sources, the phase relationship between the fluctuating spoiler drag forces, and the ratio of the mean drag forces provide the basis of a generalized predictive technique. Further work is required to extend the work to the interactions of practical duct discontinuities such as bends and transition pieces.

ACKNOWLEDGMENTS

The work described in this paper was fully supported by a grant from the Research Grants Council of the Hong Kong Special Administrative Region, China (Project No. PolyU 5229/05E).

NOMENCLATURE

- a, b = duct cross-section dimensions (m)
- A = area of the duct cross-section determined by $A=(a \times b)$ (m^2)
- A_s = face area of flat plate spoiler (m^2)
- A_c = area of the duct constriction determined by $A_c=(a \times b - r \times b)$ (m^2)
- c_0 = ambient speed of sound (m/s)
- C_D = drag coefficient
- d_{ij} = distance between the i th spoiler and the j th spoiler (m)
- f_c = center frequency of measurement band (Hz)
- f_0 = cut-on frequency of the first transverse duct

mode (Hz) defined by $f_0 = (c_0/2\pi) \sqrt{(m\pi/a)^2 + (n\pi/b)^2}$, where $m, n = 0, 1, \dots$

$F_i(\omega)$ = magnitude of the fluctuating drag force acting on the i th spoiler (N)

\bar{F}_{zi} = mean drag force acting on the i th spoiler counted from the inlet of the air flow (N)

\bar{F}_{z1} = mean drag force acting on the first spoiler (N)

i, j = integers

I_1, I_2 = Interaction terms below and above the cut-on frequency

J_0, J_1 = zero- and first-order Bessel's functions

k = wave number

$K(S)$ = ratio of fluctuating to steady-state drag forces on the spoilers

$K^2(S)$ = square of the ratio $K(S)$

m, n = integers

M = Mach number given by $M=U/c_0$

N = number of in-duct spoilers or in-duct elements

P_s = static pressure (Pa)

ΔP_s = static pressure drop across a spoiler (Pa)

q = volume flow rate (m^3/s)

r = characteristic dimension of the in-duct element (m)

RT = reverberation time (s)

\overline{RT} = geometrical mean of reverberation time (s)

S = Strouhal number determined by $S=f_c r/U_c$

S_D = standard deviation

SPL = sound pressure level (dB)

SWL = sound power level radiated from the duct exit (dB)

U = mean duct flow velocity (m/s)

U_c = flow velocity in the constriction (m/s) determined by $U_c=q/A_c=UA/A_c$

V_R = room volume of the reverberation chamber (m^3)

ω_c = center radiant frequency of the measurement band (rad/s)

Π = sound power (W)

Π_N = infinite-duct values of the radiated sound power due to multiple (N) spoilers (W)

Π_S = infinite-duct values of the radiated sound power due to an in-duct spoiler (W)

Γ_1, Γ_2 = power terms from the first spoiler below and above the cut-on frequency (W)

ρ_0 = ambient air density (kg/m^3)

σ = open area ratio determined by $\sigma=A_c/A$

γ_{ij}^2 = coherence function of the i th spoiler and the j th spoiler

$\phi_{ij}(\omega_c)$ = phase of the cross-power spectral density of the source volume of the i th sound source and the j th sound source

ζ_i = constant ratio of the mean drag forces acting on the i th spoiler and the first spoiler

β_N = interaction factor

$\phi_{ij}(\omega_c)$ = phase of the cross-power spectral density of the source volume of the i th sound source and the j th sound source
 δ_{ij} = difference between the phases of the total fluctuating drag forces acting on the i th spoiler and the j th spoiler determined by $\delta_{ij} = \theta_j(\omega) - \theta_i(\omega)$, where $\theta_i(\omega)$, $\theta_j(\omega)$ phases of the fluctuating drag force acting on the i th spoiler and the j th spoiler, respectively.

¹ASHRAE (American Society of Heating, Refrigerating and Air-Conditioning Engineers) Handbook, HVAC Applications SI Edition, 47.7–47.10 (American Society of Heating, Refrigerating and Air-Conditioning Engineers, Inc., 2007).

²CIBSE (The Chartered Institution of Building Services Engineers) guide B5 Noise and Vibration Control for HVAC, 7–9 (The Chartered Institution of Building Services Engineers London, May 2005).

³T. K. Wilson and A. Iqbal, "Computer-aided analysis of airflow systems noise," *Build. Services Eng. Res. Technol.* **1**, 54–57 (1980).

⁴U. Ingard, A. Oppenheim, and M. Hirschorn, "Noise generation in ducts," *ASHRAE Trans.* **74** (1968).

⁵W. W. Soroka, *Refriger. Eng.* **37**, 393 (1939).

⁶W. W. Soroka, "Experimental study of high velocity air discharge noise from some ventilating ducts and elbows," *Appl. Acoust.* **3**, 309–321 (1970).

⁷W. F. Kerka, "In high velocity system duct parts create sound as well as suppress it," *ASHRAE J.* **429**, 49–54 (1960).

⁸J. H. Watson, "Acoustical characteristics of mitre bends with lined turning vanes," *Australian Refrigeration, Air Conditioning & Heating* **22**, 30–33 (1968).

⁹H. Brockmeyer, "Flow acoustic study of duct fittings of high velocity air conditioning systems," Ph.D. dissertation for degree of Dr.-Ing. Carolo Wilhelmina, Technical University, Braunschweig, HVRA (The Heating & Ventilating Research Assoc.) Translation 195, 1968.

¹⁰J. B. Chaddock, "Ceiling air diffuser noise," Technical Information Report No. 45. Bolt Beranek and Newman Inc., Boston, MA, 1957.

¹¹M. Hubert, "Noise development in ventilation plant," *Larmbekämpfung* **46–51**, 29–33 (1969).

¹²M. J. Holmes, "Air flow generated noise Part II: Bends with turning vanes," *Proceedings of the Institute of Acoustics, Laboratory Report No. 78*, The Heating & Ventilating Research Association, Blacknell, UK, 1973.

¹³C. G. Gordon, "Spoiler-generated flow noise. I: The experiment," *J. Acoust. Soc. Am.* **43**, 1041–1048 (1968).

¹⁴C. G. Gordon, "Spoiler-generated flow noise. II: Results," *J. Acoust. Soc. Am.* **45**, 214–223 (1969).

¹⁵H. H. Heller and S. E. Widnall, "Sound radiation from rigid flow spoilers correlated with fluctuating forces," *J. Acoust. Soc. Am.* **47**, 924–936 (1970).

¹⁶P. A. Nelson and C. L. Morfey, "Aerodynamic sound prediction in low speed flow ducts," *J. Sound Vib.* **79**, 263–289 (1981).

¹⁷D. J. Oldham and A. U. Ukpoho, "A pressure-based technique for predicting regenerated noise levels in ventilation systems," *J. Sound Vib.* **140**, 259–272 (1990).

¹⁸A. U. Ukpoho and D. J. Oldham, "Regenerated noise levels due to closely spaced duct elements," *Proceedings of Institute of Acoustics* **13**, 461–468 (1991).

¹⁹M. M. Zdravkovich, "Review of flow interference between two circular cylinders in various arrangements," *J. Fluids Eng.* **99**, 618–633 (1977).

²⁰C. M. Mak and J. Yang, "A prediction method for aerodynamic sound produced by closely spaced elements in air ducts," *J. Sound Vib.* **229**, 743–753 (2000).

²¹C. M. Mak and J. Yang, "Flow-generated noise radiated by the interaction of two strip spoilers in low speed flow ducts," *Acta. Acust. Acust.* **88**, 861–868 (2002).

²²C. M. Mak, "Development of a prediction method for flow-generated noise produced by duct elements in ventilation systems," *Appl. Acoust.* **63**, 81–93 (2002).

²³C. M. Mak and D. J. Oldham, "The application of computational fluid dynamics to the prediction of flow generated noise in low speed ducts. Part 1: Fluctuating drag forces on a flow spoiler," *Build. Acoust.* **5**, 123–141 (1998).

²⁴C. M. Mak and D. J. Oldham, "The application of computational fluid dynamics to the prediction of flow generated noise in low speed ducts. Part 2: Turbulence-based prediction technique," *Build. Acoust.* **5**, 199–213 (1998).

²⁵C. M. Mak, "Prediction methods for regenerated noise produced by two elements in an air duct," *Build. Acoust.* **8**, 187–192 (2001).

²⁶C. M. Mak and W. M. Au, "A turbulence-based prediction technique for flow-generated noise produced by in-duct elements in a ventilation system," *Appl. Acoust.* **70**, 11–20 (2009).

²⁷C. M. Mak, "A prediction method for aerodynamic sound produced by multiple elements in air ducts," *J. Sound Vib.* **287**, 395–403 (2005).

²⁸N. Han, X. J. Qiu, and C. M. Mak, "A further study of the prediction method for aerodynamic sound produced by two in-duct elements," *J. Sound Vib.* **294**, 374–380 (2006).

²⁹N. Han and C. M. Mak, "Prediction of flow-generated noise produced by acoustic and aerodynamic interactions of multiple in-duct elements," *Appl. Acoust.* **69**, 566–573 (2008).

³⁰ASTM (American Society for Testing and Materials) Standard: D 3154 Standard test method for average velocity in a duct (Pitot tube method), An American National Standard (ASTM, November 2000).